Development of a Butterfly-style Flapping Robot with a Different Ratio of Down and Up Stroke Times

Taro FUJIKAWA*1 and Koki KIKUCHI*2

*1 Department of Robotics and Mechatronics, Tokyo Denki University
5 Senju, Asahi-cho, Adachi-ku, Tokyo, 120-8551, JAPAN
fujikawa@fr.dendai.ac.jp

*2 Department of Advanced Robotics, Chiba Institute of Technology
2-17-1 Tsudanuma, Narashino-city, Chiba, 275-0016, JAPAN
kikut@ieee.org

Abstract

In this paper, we develop a butterfly-style flapping robot that has different timings between down and up strokes, which are based on a stroke cycle of a butterfly. A butterfly flies upward during the down stroke and forward during the upstroke using posture control; this trajectory resembles a staircase pattern. One of the causes of these flight characteristics is the ratio between the time periods of the down and up strokes. We developed a mechanism to mimic this stroke cycle that is based on a quick-return mechanism and validated it via motion analysis and numerical simulation. The results indicate that this quick-return mechanism is useful for a flapping robot that needs simplicity to achieve a minimal payload for flight. Furthermore, the ratio of the strokes affected both the body pitch angle and trajectory during the flight.

Keywords: flapping robot, down stroke time, up stroke time, body pitch angle

1 Introduction

In recent years, flying robots such as multi-rotor helicopters have been actively developed for practical applications [1 - 4]. Although, the size of these common flying robots ranges from several tens of centimeters to a few meters, it is desirable that the size of the robots decreases so as to let it pass through narrow spaces. From this viewpoint, flapping robots modeled after small bird such as humming-birds [5, 6] or insect such as flies [7-10] have been developed. However, these robots have not achieved practical flight because it is difficult to implement a battery, complex link mechanisms, and actuators that drive wings and control postures within such a small body. One of the problems to overcome is the method of posture control. Although insects control their posture during flight by flapping, lead-lag, and feathering of the wings, it is difficult to actualize these motions in insect-scale robots as described above. Therefore, constructing a posture control system in a simple and lightweight manner is necessary to achieve practical flight in small flapping robots.

To overcome such challenges, we have developed a small flapping robot modeled after a butterfly that has a low flapping frequency of approximately 10Hz and a few degrees of freedom of the wings [11]. The flapping robot is similar in size to that of a butterfly, i.e., its wingspan is almost 100mm, wing chord length is 45mm, and total mass, including an actuator, is less than 500mg. Our flapping robot has a large flapping angle of 80deg to -60deg and a mechanism that realizes both flapping and lead-lag motion by an actuator. These allow the flapping robot to take off from an airspeed of 0m/s and fly upward during the down stroke and then forward during the up stroke, which occurs in a staircase pattern that mimics the flight trajectory of a butterfly. Furthermore, we investigated the flight characteristics of different flapping and initial body pitch angles for posture control by performing hardware experiments and numerical simulations [12]. We then shed light on the difference in the timing between the down strokes and up strokes in a flapping butterfly. Specifically, it is thought that the ratio between the timings of the down and up strokes affects the posture control of a butterfly.

This paper is organized as follows: In section 2, we describe a butterfly-style flapping robot with a mechanism to generate a difference between the down and up stroke times. In section 3, we demonstrate the stroke mechanism by physical experiments. In section 4, we analyze the flight characteristics for different ratios of the down and up strokes via numerical simulations. Finally, in section 5, we conclude the paper and outline future work.

2 Butterfly-style flapping robot

2.1 Flight characteristics of a butterfly

Figure 1 shows a swallowtail butterfly (*Papilio xuthus*) as a model for a flapping robot and a typical takeoff motion captured by high-speed camera (DITECT Co., Ltd.). The red line in Fig. 1 denotes the trajectory of the center of the thorax. To investigate the flight characteristics of a butterfly, we focus on the relationship between flapping and body pitch angles. Definitions of these angles are shown in **Fig. 2**.

Figure 3 shows the flapping and body pitch angles during takeoff. The flapping frequency was approximately 10Hz, and the time of the down stroke was 65ms and that of the up stroke was 40ms. This shows that the ratio between down and up strokes is approximately 1.5. Furthermore, the body pitch angle increased after the flapping angle reached 0deg during

the down stroke and then decreased after the flapping angle reached 0deg during the up stroke. Thus, this is why it is hypothesized that controlling the ratio of the strokes cycles makes it possible to change body pitch angle that affects its posture.

Fig. 1 Butterfly as a model (left) and an example of successive picture during takeoff (right)

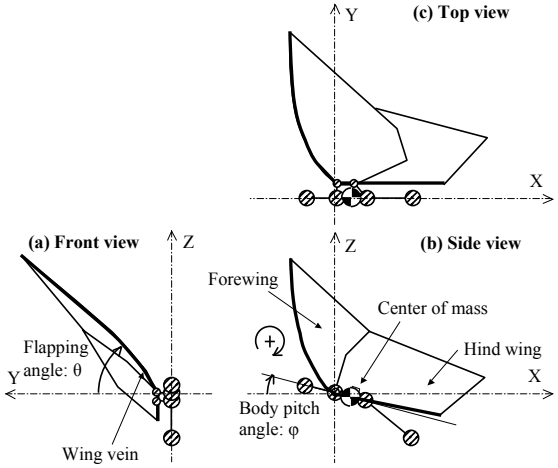

Fig. 2 Definition of butterfly model parameters

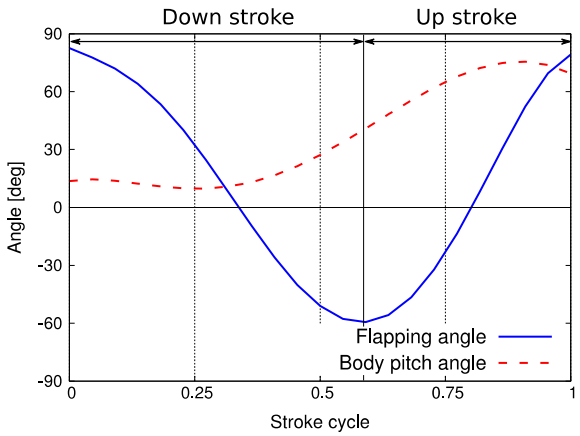

Fig. 3 An example of flapping and body pitch angles during takeoff of a butterfly

2.2 Flapping mechanism for different stroke ratio

In order to generate the difference between down and up stroke times, we made a simple quick-return mechanism as shown in **Fig. 4**. This mechanism is constructed of three links. Link 1 rotates at a constant frequency and link 3 swings up and down. The time of these up and down motion depends on the angle between link 1 and link 2, i.e., the ratio of α to β in Fig. 4. For example, if the ratio of α to β is 1/2 and the rotational direction of link 1 is clock-wise, the ratio between up and down stroke times of link 3 is 1/2.

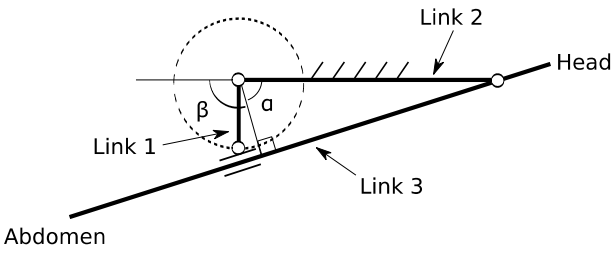

Fig. 4 Quick return mechanism for butterfly model

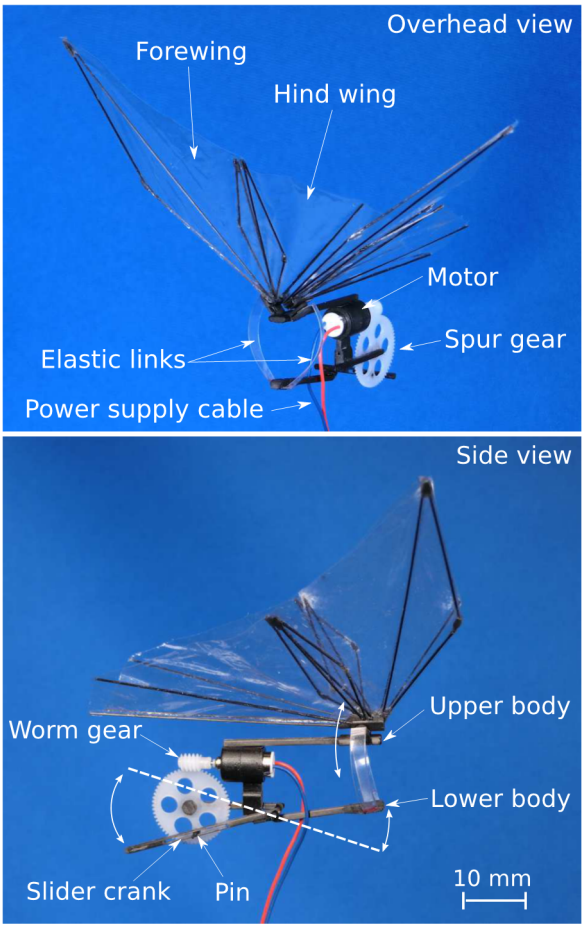

Fig. 5 Manufactured flapping robot without battery

2.3 Development of a flapping robot

We developed the butterfly-style flapping robot based on our prior robot [11]. The robot as shown in **Fig. 5** is constructed of CFRP (carbon fiber reinforced plastic) in order to be lightweight and have high rigidity, and is equipped with a 4mm coreless motor. The wing membranes are 2 micrometer thick films made of polyethylene. The quick return mechanism consists of a spur gear (module 0.2) and a lower body. Link 1 corresponds to the length between center of spur gear and pin in Fig. 4, and link 3 corresponds to the lower body. The swing motion of the lower body generates flexural deformation of the elastic links. This deformation generates a flapping motion of the wings. We adopted viewgraphs for these elastic links because it has moderate elasticity and ready availability. The amount of flexure of an elastic link depends on the amount of swing movement of the lower body; the details have been previously documented [11]. The wingspan and wing chord length are 114mm and 44mm, respectively. The robot has a total mass of 1.6g, which includes a Li-Po battery (3.7V, 30mAh). The ratio between down and up stroke times was set to 1.5 based on the above analysis of a butterfly.

3 Experiments of flapping mechanism

To demonstrate the capability of the mechanism to generate different down and up stroke times, we analyzed the flapping motion of the robot by high-speed camera (1280 × 1024pixels and 1000fps, DITECT Co., Ltd.). In this experiment, the robot was fixed on a support pole to deaden the vibrations of the body by its flapping wings.

Figure 6 displays stroboscopic images of the robot during a stroke. The down stroke was from 0 to 49ms and the up stroke was from 49 to 83ms. The flapping angle is shown in **Fig. 7** for two stroke cycles. Although the amplitude of both down and up stroke angles were low compared with a butterfly, the ratio between down and up strokes is similar to that of a butterfly. This result showed that this quick-return mechanism could be effective for butterfly-style flapping robots.

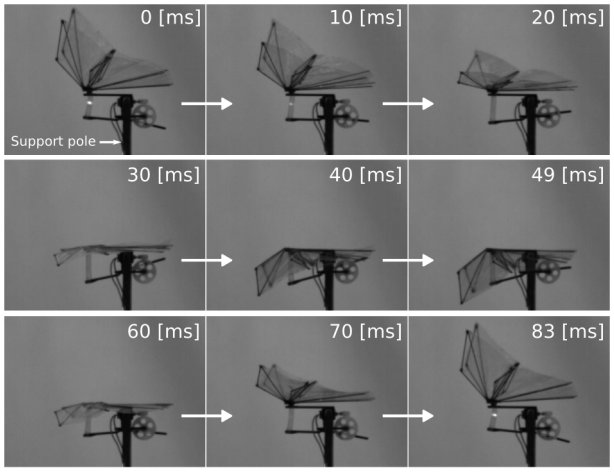

Fig. 6 Stroboscopic photographs of a development robot captured during one stroke cycle

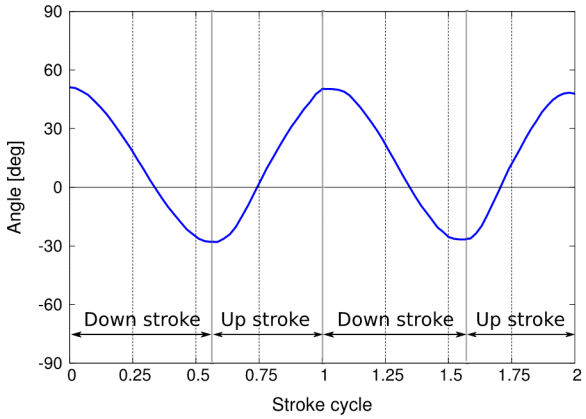

Fig. 7 Flapping angle of a butterfly robot during two stroke cycles

4 Numerical simulations for flight characteristics

4.1 Simulation models

To clarify the flight characteristics for different ratios of down and up strokes of a butterfly, we performed numerical simulations, and **Fig. 8** outlines the simulation model. The body consists of four mass points that are connected by springs and dampers, which are the head, thorax 1, thorax 2, and abdomen. Both right and left wings have their respective fore and hind wings integrated for synchronous movement. Each of masses and lengths is calculated by observed value of butterflies. The coefficients of each springs and dampers are set by qualitative estimate of the motion of butterflies. The finite element method was used to calculate the body and wing motions and flow fields around the wings; the details have been previously documented [13]. This simulation model is possible to analyze flight characteristics of a butterfly, such as flight trajectory and shift in posture during a flight.

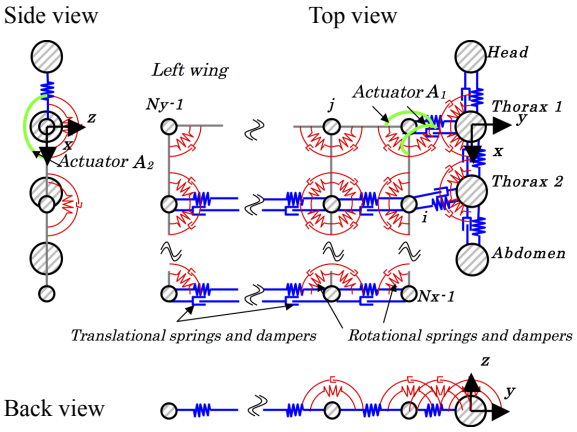

Fig. 8 Butterfly robot simulation model

4.2 Setting parameters

In this study, to clarify the relationship between the ratio of down and up stroke times and body pitch angle, we used three models. The ratios between down and up

strokes of models A, B, and C are 1.5, 1.0, and 0.67, respectively. Each model has flapping angles of 70deg to -60deg, an initial body pitch angle of 0deg, and a flapping frequency of 12Hz. The wingspan and the wing chord length of each model are 118mm and 45mm, and the total mass of each model, including an actuator, is 500mg, which is equivalent to that of a butterfly. **Table 1** shows these experimental parameters.

Table 1 Butterfly robot simulation parameters

	Model A	Model B	Model C
Flapping angle [deg]	70 to -60	70 to -60	70 to -60
Flapping frequency [Hz]	12	12	12
Down/Up stroke cycle ratio	1.5	1.0	0.67

4.3 Results and discussion

Figure 9, **10**, and **11** show comparisons of flapping and body pitch angles of models A, B, and C, respectively. **Figure 12** shows a comparison of the trajectories of the center of masses of the three models.

There was tendency that body pitch angle increased during the down stroke and decreased during the up stroke in each model. However, the body pitch angles of models A and B showed a general increasing tendency, and in contrast to this, Model C showed a decreasing tendency. Now, we will focus on the end of the first and second strokes. The body pitch angle of Model A (12.3deg and 71.7deg) were both larger than that of models B (6.6deg and 43.4deg) and C (-5.4deg and -34.1deg). In case of model C, it was a negative value, i.e., the posture of Model C is in a nose down condition. In fact, when the ratio was high the nose up movement became larger than the nose down movement during a cycle. In contrast to this, when the ratio was low, the nose down movement became larger than the nose up movement during a cycle. It can be see that Model A is flying upward the end of the second stroke, and Model C is flying downward at the end of the second stroke, shown in Fig. 12. We now focus on the soar height of the first down stroke for each model. Model C flew higher than models A and B. The maximum height during the first stroke of models A, B, and C were 24.6, 32.3, and 41.3mm, respectively. This shows that the lower the ratio between down and up stroke times became the higher the flapping robot flew. This is due to the reaction force of the wings becoming larger in proportion to the flapping speed. In case of Model C, the flying distance during the down stroke was longer than that of models A and B. In contrast to this, the flying distance of Model A during the up stroke was longer than that of models B and C.

To verify the reaction force on the wings, we fabricated a robot of Model C, and investigated the stress distribution in its wing by using a polarized high-speed camera (1024 × 1024pixels and 1000fps, PHOTRON LIMITED). This camera is possible to measure birefringence by polarized light and analyze stress distribution [14]. Note that, in this experiment, the fore and hind wings were integrated as in the numerical simulation.

Figure 13 shows the stress distribution in the right wing at the moment of almost 0deg during both down and up strokes. The color is a heat map that represents the amount of stress on the wings, i.e., red denotes higher and blue denotes lower stress. This shows that the stress during the down stroke was higher throughout the whole of the wing compared with that during the up stroke. This is because the flapping speed of the down stroke was faster than that of the up stroke in Model C. Therefore, this increased stress is consistent with more reaction force during the down stroke and is why Model C flew higher during down stroke compare with models A and B. These results showed that it is possible to control body pitch angle and flying height by changing the ratio between down and up strokes times for a butterfly-style flapping robot. Furthermore, since the elastic deformation of the wing affects generation of the lift for flapping movement, we consider that the stress distribution of the wing is important to design of the wing of a robot. Therefore, in future works, we will clarify this effect for flight characteristics and validate it by performing experiments of the robots. We will change the stress distribution of its wings by varying configurations and thickness of wing veins.

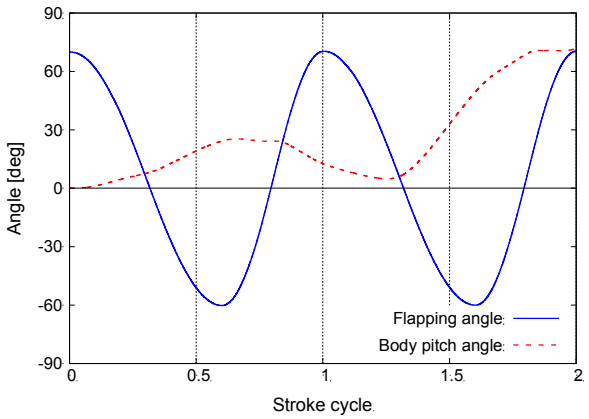

Fig. 9 Relationship between flapping and body pitch angles during takeoff of Model A

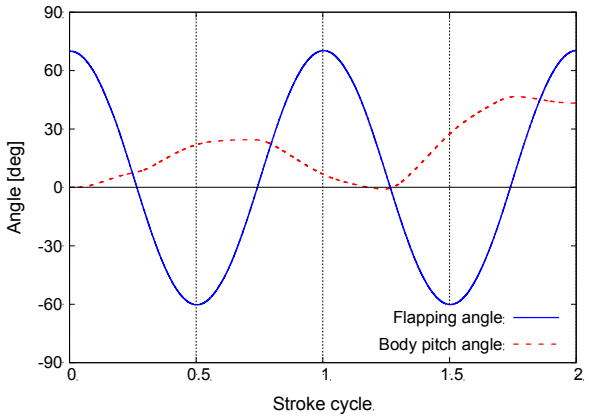

Fig. 10 Relationship between flapping and body pitch angles during takeoff of Model B

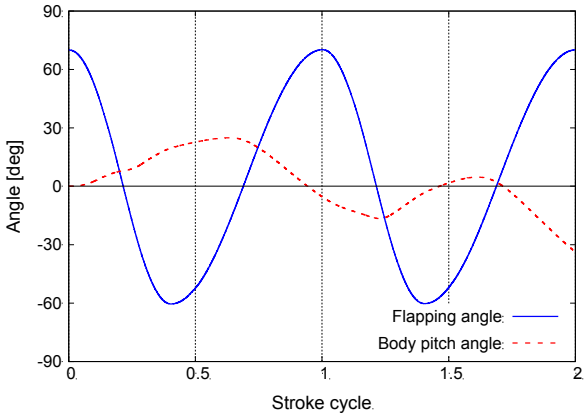

Fig. 11 Relationship between flapping and body pitch angles during takeoff of Model C

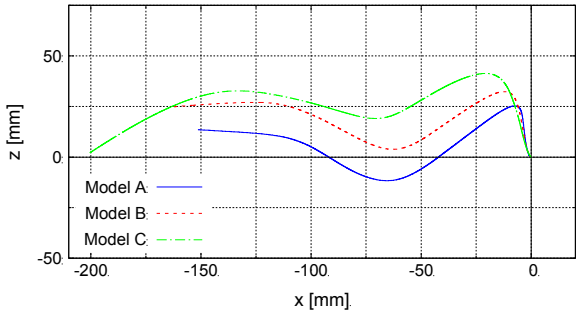

Fig. 12 Transitions of center of mass of models A, B, and C during takeoff (direction of movement is negative direction of x-axis based on Fig. 8)

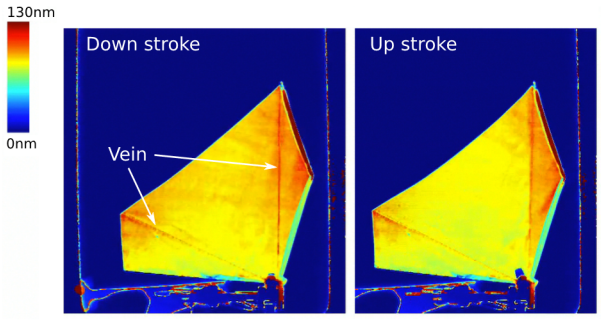

Fig. 13 An example of stress distribution in a right wing of Model C (flapping angle is around 0 deg) captured by polarized high-speed camera

5 Conclusions

To realize posture control of a butterfly-style flapping robot, we developed a quick-return mechanism that made it is possible to change the ratio between down and up stroke times, which were chosen based on an analysis of a butterfly. Furthermore, we demonstrated the validity of the mechanism by performing experiments and analyzing the flight characteristics by using numerical simulations.

Our previous research showed that these flight characteristics were also possible to control by different flapping or initial body pitch angles. Therefore, it is believed that we are able to develop a butterfly-style flapping robot that is easier to control by a combination of parameters, such as flapping angle, initial body pitch angle, and the ratio between down and up stroke times.

In future research, we aim to validate the effect of different ratios between down and up stroke times by performing flight experiments of robots and analyzing the lift and body pitch movements quantitatively.

Acknowledgements

The authors are grateful to T. Oonuma, K. Ikuo, and M. Ito of Photron ltd. for technical assistance with the experiments of stress distribution in subsection 4.3.

This research was partially supported by Research Institute for Science and Technology of Tokyo Denki University Grant Number Q15T-09/Japan.

References

[1] E. W. Green and P. Y. Oh, “Autonomous Hovering of a Fixed-Wing Micro Air Vehicle,” Proceedings of 2006 IEEE International Conference on Robotics and Automation, (2006), pp. 2164-2169.

[2] G. Hoffman, H. Huang, et al., “Quadrotor Helicopter Flight Dynamics and Control: Theory and Experiment,” Proceedings of 2007 International Conference on the American Institute of Aeronautics and Astronautics, (2007), pp. 1-20.

[3] M. Whitzer, J. Keller, S. Bhattacharya, V. Kumar, “In-Flight Formation Control for a Team of Fixed-Wing Aerial Vehicles,” Proceedings of 2016 International Conference on Unmanned Aircraft Systems, (2016), pp. 372-380.

[4] K. Nonami, “Drone Technology, Cutting-Edge Drone Business, and Future Prospects,” Journal of Robotics and Mechatronics, Vol. 28, No. 3, (2016), pp. 262-272.

[5] H. Liu and H. Aono “Size effects on insect hovering aerodynamics: an integrated computational study,” Bioinspiration and Biomimetics, Vol. 4, No. 1, (2009), pp. 1-13.

[6] M. Karásek, Y. Nan, I. Romanescu, and A. Preumont, “Pitch Moment Generation and Measurement in Robotic Hummingbird,” International Journal of Micro Air Vehicles,Vol. 5, No. 4, (2013), pp. 299-309.

[7] R. S. Fearing, K. H. Chiang, M. H. Dickinson, D. L. Pick, M. Sitti, and J. Yan, “Wing Transmission for a Micromechanical Flying Insect,” *proceedings of IEEE International Conference on Robotics and Automation*, (2000), pp. 1509-1516.

[8] M. Sitti, “PZT Actuated Four-Bar Mechanism with Two Flexible Links for Micromechanical Flying Insect Thorax,” *proceedings of IEEE International Conference on Robotics and Automation*, (2001), pp. 3893-3900.

[9] R. J. Wood, “The First Takeoff of a Biologically Inspired At-Scale Robotic Insect,” *IEEE Trans. Rob.*, Vol. 24, No. 2, (2008), pp. 341-347.

[10] P. Chirarattananon, K. Y. Ma, and R. J. Wood, “Adaptive Control for Takeoff, Hovering, and Landing of a Robotic Fly,” International Conference on Intelligent Robots and Systems, (2013), pp. 3808-3815.
[11] T. Fujikawa, Y. Sato, T. Yamashita, and K. Kikuchi, “Development of A Lead-Lag Mechanism Using Simple Flexible Links for A Small Butterfly-Style Flapping Robot,” ISIAC2010, (2010).
[12] T. Fujikawa, M. Shindo, and K. Kikuchi, “Motion Analysis of Pitch Rotation Mechanism for Posture Control of Butterfly-style Flapping Robot,” JSDE The 3rd International Conference on Design Engineering and Science, (2014), pp.84-89.
[13] T. Fujikawa, *et al.*, “Development of a Small Flapping Robot -Motion Analysis during Takeoff by Numerical Simulation and experiment-,” Mechanical Systems and Signal Processing (MSSP), Vol.22, No.6, (2008), pp.1304-1315.
[14] T. Onuma and Y. Otani, “A development of two-dimensional birefringence distribution measurement system with a sampling rate of 1.3 MHz,” Optics Communications, Vol. 315, No. 15, (2014), pp.69-73.

Received on January 13, 2017
Accepted on March 21, 2017